Heat Transfer Behaviors of Thermal Energy Storages for High Temperature Solar Systems

A. Andreozzi, B. Buonomo, O. Manca, S. Nardini and S. Tamburrino

Abstract Solar energy is an important alternative energy source that will likely be utilized in the future. One main limiting factor in the application of solar energy is its cyclic time dependence. Therefore, solar systems require energy storage to provide energy during the night and overcast periods. Although the need of thermal energy storage also exists for many other thermal applications, it is particularly notable for solar applications. It can improve the efficient use and provision of thermal energy whenever there is a mismatch between energy generation and use. In sensible thermal storage, energy is stored by changing the temperature of a storage medium. The amount of energy input to thermal energy storage by a sensible heat device is proportional to the difference between the storage final and initial temperatures, the mass of storage medium and its heat capacity. Each medium and porous matrix has its own advantages and disadvantages.

A. Andreozzi (✉)
Dipartimento di Ingegneria Industriale, Università degli Studi di Napoli Federico II, Piazzale Tecchio 80 80125 Naples, Italy
e-mail: assunta.andreozzi@unina.it

B. Buonomo · O. Manca · S. Nardini · S. Tamburrino
Dipartimento di Ingegneria Industriale e dell'Informazione, Seconda Università degli Studi di Napoli, Via Roma 29 81031 Aversa, CE, Italy
e-mail: bernardo.buonomo@unina2.it

O. Manca
e-mail: oronzio.manca@unina2.it

S. Nardini
e-mail: sergio.nardini@unina2.it

S. Tamburrino
e-mail: salvatore.tamburrino@unina2.it

Nomenclature

a_{sf}	Specific surface area, m^{-1}
c, c_p	Specific heat, $Jkg^{-1}K^{-1}$
C	Inertia coefficient
d_p	sphere diameter
D	Cylinder diameter, m
G	Mass velocity, $kg\ m^{-2}\ s^{-1}$
h	Surface heat transfer coefficient, $Wm^{-2}K^{-1}$
h_{sf}	Interfacial heat transfer coefficient between solid matrix and fluid, $Wm^{-2}K^{-1}$
H	Height of the cross section, m
k	Thermal conductivity, $Wm^{-1}K^{-1}$
K	Permeability, m^{-2}
L	Cylinder height, channel length, m
m	Mass flow rate, $kg\ s^{-1}$
p	Pressure, Pa
Pr	Prandtl number
q	Heat flux, Wm^{-2}
r, z	Cylindrical coordinates, m
Re	Reynolds number
s	Channel thickness, m
t	Time, s
T	Temperature, K
u, v	Velocity component, ms^{-1}
x, y, z	Cartesian coordinates, m

Greek

ε	Emissivity coefficient
φ	Porosity
μ	Dynamic viscosity, Pa s
ρ	Density, kgm^{-3}

Subscripts

f	Fluid
in	Initial
p	Porous
s	Solid

1 Introduction

Energy storage not only plays an important role in the energy conservation but also improves the performance and reliability of wide range of energy systems, and becomes more important where the energy source is intermittent such as solar. Energy storage process can reduce the rate mismatch between energy supply and energy demand. Devices for the energy conservation and management are largely employed in many industrial and commercial applications to supply thermal energy, if it would be needed. Energy demands in the commercial, industrial and utility sectors vary on daily, weekly and seasonal bases. These demands can be matched thanks to thermal energy storage (TES) systems that operate synergistically. TES for thermal applications, such as space and water heating, cooling, air-conditioning, etc., has recently received much attention [1–9]. A storage system therefore constitutes an important component of the solar energy utilization system.

Solar energy is an important alternative energy source that will likely be utilized in the future. One main limiting factor in the application of solar energy is its cyclic time dependence. Therefore, solar systems require energy storage to provide energy during the night and overcast periods. A line diagram of a typical solar energy utilization system is shown in Fig. 1 [10]. Thermal energy can be stored as sensible heat, latent heat or chemical energy. An overview of major technique of storage of solar thermal energy is shown in Fig. 2 [11]. In sensible heat storage, heat is stored by increasing the storage medium temperature. In case of latent heat storage systems, the energy is stored in phase change materials. The heat is stored when the material changes phase from solid to a liquid. Thermo-chemical storage is a technique, which involves chemical reactions.

Since the first oil crisis of the 1970s, concentrated solar power (CSP) generation has become a promising alternative to conventional electricity production. Contrary to other renewable energy technologies like photovoltaic or wind power, CSP offers the advantage of thermal energy storage (TES), which allows for electricity production on demand and independently of the solar resource. The most widespread CSP technology is the parabolic trough system, where parabolic mirrors are used to concentrate sunlight onto an absorber tube located at the focus line. A heat transfer fluid (HTF) circulates in thousands of meters of lighted pipes to collect the thermal energy and then transfer it to a steam generator via a heat exchanger.
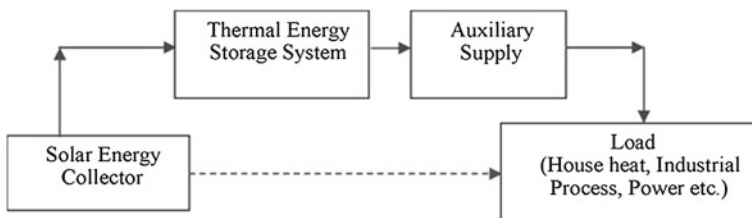

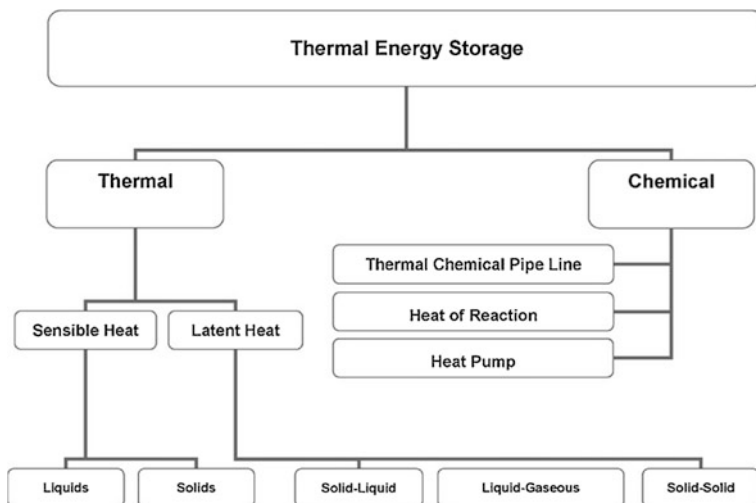**Fig. 1** Line diagram for a solar energy utilization system [10]

Fig. 2 Overview of thermal energy storage systems [11]

TES in concentrated solar power (CSP) technology is very important to deliver high-temperature heat in the form of sensible heat storage in a packed bed of rocks or other ceramic materials and it is especially suitable when a gas is used as the heat transfer fluid in the solar receiver [10–15]. However, some other types of porous media such as ceramic foams or honeycomb could be employed as material for High Temperature Thermal Energy Storage (HTTES) unit to realize a different sensible heat storage system with lower thermal capacity and pressure drop [4, 12, 16].

Thermal energy storage systems for concentrated solar power (CSP) plants have featured the use of molten salt [17, 18], steam [19], and concrete [20] for sensible heat, phase change materials for latent heat [19], and reversible reactions for thermochemical storage [12, 20, 21]. The use of a packed bed of rocks as sensible heat storing material and air as heat transfer fluid was studied in [22]. This method of storage concept is incorporated in solar power plants using air as working fluid [23, 24]. Its main advantages are: (a) abundant and economical storing material; (b) applicability in a wide temperature range, with limiting temperatures given by the rock's melting point; (c) direct heat transfer between working fluid and storage material; (d) no degradation or chemical instability; (e) no safety concerns, and (f) elimination of chemicals and corrosive materials.

A packed bed storage system consists of loosely packed solid material through which the heat transport fluid is circulated. Heated fluid, usually air, flows from solar collectors into a bed of graded particles from top to bottom and thermal energy is transferred from the fluid to the particles during the charging phase. Packed bed, generally, represents the most suitable energy storage unit for air based solar systems as mentioned by Coutier and Farber [25]. During the charging phase, solar heated air is forced into the top of the container, i.e., upper plenum

and then passes evenly down through the bed heating the storage and passes out through the lower plenum. Air is drawn off at the bottom and returned to the solar collectors. When energy is needed from storage, the airflow is reversed. However, some other type of porous media such as ceramic foams or honeycomb could be employed as material in the storage unit to realize a different storage system with lower thermal capacity and pressure drop.

Several investigations describe numerical simulation models for sensible heat storage in porous media [16].The heat transfer to and from a flowing fluid to a packed bed has been the subject of many theoretical and experimental researches since Schumann's original work [26]. A one-dimensional two-phase model for packed bed system was assumed by ignoring the thermal capacity of the fluid, axial conduction both in the fluid and in the bed material. Some elaborations were performed in [27–29] to facilitate the extraction of numerical information from the solutions by providing nomograms, extensive graphs and tabulations. Numerical simulations were carried out to solve the governing equations for the packed bed by finite difference methods [30–32]. A mathematical model to evaluate the dynamic response of a packed column to an arbitrary time dependent inlet air temperature was accomplished in [33]. Different aspects of sensible heat storage systems were analyzed in [34]. It was reported that the preference of sensible heat storage system depends upon the storage period, economical viability and operating conditions. An investigation on different energy storage techniques and materials employed in sensible heat storage systems was accomplished in [35]. A comparative numerical study on packed bed thermal models suitable for sensible and latent heat thermal storage systems was presented in [36]. Four basic groups of models were investigated and the models were compared in relation to the influence of particle size, void fraction, particle material, flow rate variations, working fluid inlet temperature variations and wall thermal losses.

A method of preserving the stratification by segmenting the storage bed was numerically studied in [37]. In fact, segmenting a standard rock bed and routing the flow to segments cooler than the inlet air during charging was shown to preserve stratification throughout the bed. An experimental investigation on heat transfer and pressure drop characteristics of packed bed solar energy storage system with large sized elements of storage material was presented in [38]. Correlations were developed for Nusselt number and friction factor as function of Reynolds number, roundness and void fraction. An extensive literature review of research work on packed bed systems was presented in [10]. The effect of multiple charge and discharge cycles was studied in detail in [39]. The amplitude of temperature fluctuation, a parameter relating to the energy storage, was seen to vary significantly with distance and time. A high temperature TES was numerically parametrically analyzed by using CFD code to solve the governing equation in porous media in transient regime [40]. High temperature TES in a packed bed of rocks was studied in [13] for air-based concentrated solar power plants. A 1-D porous medium model in local thermal non equilibrium was assumed and two-phase energy conservation equations for combined convection and conduction heat transfer were solved numerically for charging/discharging cycles. A comparison

between numerical results and their experimental data was accomplished for a packed bed of crushed steatite (magnesium silicate rock) at 800 K. A thermal energy storage system, consisting of a packed bed of rocks as storing material and air as high-temperature heat transfer fluid, was analyzed for concentrated solar power (CSP) applications in [8].

The honeycomb structure is used in many applications such as heat storage, heat regenerators, drying and cooling of electronic equipment [8, 12, 14, 41–49]. A micro-cell aluminum honeycomb employed in augmenting heat transfer in compact heat exchangers was investigated by an analytical model in [41]. For convective cooling, the overall heat transfer rate was found to be elevated by about two order of magnitudes when an open channel was designed with an aluminum honeycomb core. A two-dimensional numerical simulation model to solve fluid-dynamic and thermal problem in a composite honeycomb regenerator was developed in [42]. Dynamic temperature and velocity profiles of gases and solid heat-storing materials were carried out. The energy storage was calculated and thermal performance of honeycomb heat regenerator was evaluated at different switching times and loading. A honeycomb reactor obtained by the assembling of several cavities, in order to optimize a thermo-chemical reactor for hydrogen production or high temperature heat storage, was analyzed in [43]. A simplified method to evaluate the optimized solar thermo-chemical reactor geometry also considering radiation in the cavity and conduction inside the reactive material was proposed. A honeycomb porous microchannel cooling system for electronics cooling was proposed and experimentally investigated in [44]. The design, fabrication, and test system configuration of the microchannel heat sink were reported. The experimental results allowed to conclude that the considered cooling system is able to perform heat dissipation well. A numerical investigation on a two-dimensional model for predicting heat and mass transfer in an alanate hydride reactor with metallic honeycomb structure heat exchanger was accomplished in [45]. Heat transfer process in honeycomb ceramics systems to estimate the effects of temperature difference and hole side length on heat transfer and the resistance losses was numerically investigated in [46]. The results showed that the temperature difference between the gas and honeycomb ceramics was larger, then the heat transfer effect was better, and the resistance loss was bigger. The design and characterization of monolithic heat sinks were disclosed in [47]. The proposed heat sink geometries presented a performance enhancement relative to a conventional longitudinally finned heat sink. A multiphase transport model to simulate drying of honeycomb ceramic substrates in a conventional (hot air) drier was numerically studied in [49]. Heat and moisture transport in the honeycomb walls as well as channels were modeled. Thermal storage in a honeycomb solid matrix was numerically investigated in [50]. Moreover, ceramic foams were considered as a porous matrix in a high temperature solar thermal energy storage [51].

In the following the governing equations for porous media in Local Thermal Non-Equilibrium (LTNE) are written in cylindrical coordinate to represent a TES and three different porous matrixes are examined: packed bed with spherical

particles, foam and honeycomb with square channels. Some results are shown to compare the behaviors of the different porous matrixes employed in the thermal energy storage system.

2 Physical Problem Description and Governing Equations

A sensible heat thermal energy storage system can be considered as a container with inside a porous matrix. Several systems have a cylindrical form and the porous matrix can be set up by a packed bed or a honeycomb with square channels or a foam. In the following it will be examined a case study of a thermal energy storage. The physical system and geometry under investigation are shown in Fig. 3. It consists of a cylinder whose diameter is equal to 0.60 m and height is 1 m. The material storage is made of alumina or cordierite and it is analyzed in three different porous medium configurations: (a) packed bed with spherical particles, (b) ceramic foam or (c) honeycomb with transversal square section channels. The heat-carrying fluid is air. Thermo-physical properties of the materials are temperature independent. In some cases radiation heat transfer effect are taken into account. Heat losses with the external environment ($T_{amb} = 300$ K) are considered by setting the surface heat transfer coefficient equal to 5 W/m^{2}K.

In the porous medium region, the generalized flow model, known as the Brinkman-Forchheimer-extended Darcy model, is used in the governing equations. The conservation equations for mass, momentum and energy are, assuming a local thermal non equilibrium condition, [52–54]:

$$\frac{\partial \varphi \rho_f u_p}{\partial t} + \varphi \rho_f v_p \frac{\partial u_p}{\partial r} + \varphi \rho_f u_p \frac{\partial u_p}{\partial z} = - \varphi \frac{\partial p}{\partial z} + \varphi \mu \left(\frac{\partial^2 u_p}{\partial r^2} + \frac{1}{r} \frac{\partial u_p}{\partial r} + \frac{\partial^2 u_p}{\partial z^2} \right)$$
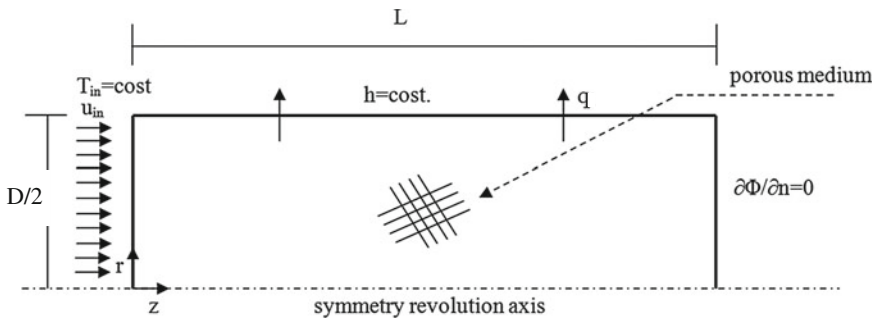$$- \varphi^2 \frac{\mu}{K} u_p - + \varphi^3 \frac{C_2 \rho_f}{2} \sqrt{u_p^2 + v_p^2} u_p \tag{1}$$

Fig. 3 Geometric configuration and physical domain

$$\frac{\partial \varphi \rho_f v_p}{\partial t} + \varphi \rho_f v_p \frac{\partial v_p}{\partial r} + \varphi \rho_f u_p \frac{\partial v_p}{\partial z} = -\varphi \frac{\partial p}{\partial r} + \varphi \mu \left(\frac{\partial^2 v_p}{\partial r^2} + \frac{1}{r} \frac{\partial v_p}{\partial r} - \frac{v_p}{r^2} + \frac{\partial^2 v_p}{\partial z^2} \right)$$
$$- \varphi^2 \frac{\mu}{K} v_p - \varphi^3 \frac{C_2 \rho_f}{2} \sqrt{u_p^2 + v_p^2} v_p$$
(2)

$$\varphi (\rho c_p)_f \frac{\partial T_f}{\partial t} + \varphi (\rho c_p)_f \left(v_p \frac{\partial T_f}{\partial r} + u_p \frac{\partial T_f}{\partial z} \right) =$$
$$\varphi k_f \left(\frac{\partial^2 T_f}{\partial r^2} + \frac{1}{r} \frac{\partial T_f}{\partial r} + \frac{\partial^2 T_f}{\partial z^2} \right) - h_{sf} a_{sf} (T_s - T_f)$$
(3)

$$(1 - \varphi)(\rho c)_s \frac{\partial T_s}{\partial t} = (1 - \varphi) k_s \left(\frac{\partial^2 T_s}{\partial r^2} + \frac{1}{r} \frac{\partial T_s}{\partial r} + \frac{\partial^2 T_s}{\partial z^2} \right) + h_{sf} a_{sf} (T_s - T_f) \quad (4)$$

where $C_2 = 2\ CK^{-0.5}$.

The permeability K and inertia coefficient C of porous medium depend on the porous matrix. The term $h_{sf} a_{sf}$ is present due to the local thermal non-equilibrium assumption and it is related with the local convective heat transfer inside the porous medium between the fluid and the solid porous matrix surfaces.

The packing of sand is best illustrated by showing the packing of uniform spheres that gives the maximum and minimum porosity, Fig. 4. The cubic packing of spheres, or in line configuration, has a porosity equal to 0.48 whereas for rhombohedral packing, or staggered configuration, the porosity is 0.26. Random packing will result in a porosity of about 0.4.

The permeability coefficient K and inertia coefficient C of porous medium, in packed bed configuration are based on these two relations [54]:

$$K = \frac{d_p^2 \varphi^3}{175(1 - \varphi)^2}, \quad C = \frac{1.75}{\sqrt{150 \varphi^{1.5}}}.$$
(5)

The convective heat transfer coefficient and the interface area per volume of packed bed [55, 56] are based on these two relations:
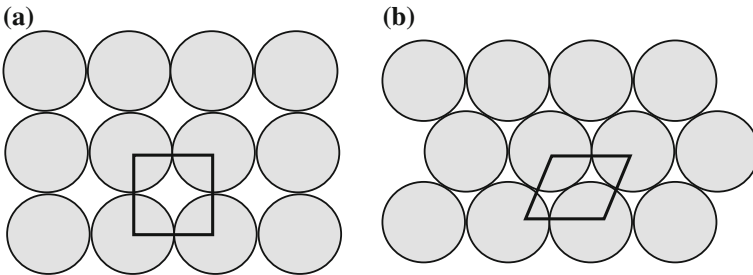

Fig. 4 Packed bed with spherical particles: **a** cubic packing, **b** rhombohedral packing

$$h_{sf} = \frac{k_f(2 + 1.1\,\mathrm{Pr}^{1/3}\,\mathrm{Re}_p^{0.6})}{d_p}; \quad a_{\mathrm{sf}} = \frac{6(1 - \varphi)}{d_p} \tag{6}$$

with

$$Re_p = \frac{|v|d_p}{v} \tag{7}$$

For ceramic foams permeability, inertia coefficient, convective heat transfer coefficient and interface area per volume of foams are evaluated by relations given in [53, 57]. Photographs of typical foam samples are shown in Fig. 5.

The radiative heat transfer was taken into account in the case of ceramic foams considering an effective thermal conductivity for the porous matrix which takes into account both heat conduction and thermal radiation as given in [58].

The permeability, K, and porosity, φ, of the considered porous medium, in honeycomb configuration, Fig. 6, are based on the following relations [55, 57].

$$K = \frac{H^4}{32(H + s)^2}; \qquad \varphi = \frac{H^2}{(H + s)^2} \tag{8}$$

where, with reference to Fig. 6, H is the width or height of the cross section of the single channel, s is the channel thickness where the thickness and the inlet section of single channel varies with the porosity. In Table 1 are given some thermophysical properties.

Convective heat transfer coefficient, h_{sf}, and interface area per volume, a_{sf}, have been evaluated numerically for single channel by means of a 3-dimensional convective steady state problem. The effect of radiative heat transfer is evaluated for the single channel and it is reported in terms of a surface heat transfer coefficient. This value is added to the convective heat transfer coefficient and employed in the evaluation of $h_{sf}a_{sf}$ coefficient. The evaluated heat transfer coefficients are summarized in Table 2 both without and with radiative heat transfer.
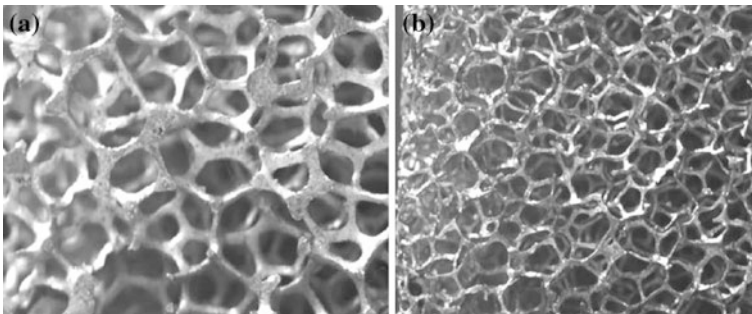

Fig. 5 Foam samples: **a** 5 PPI; **b** 40 PPI

Fig. 6 Honeycombs configuration: **a** channel, **b** square transversal section
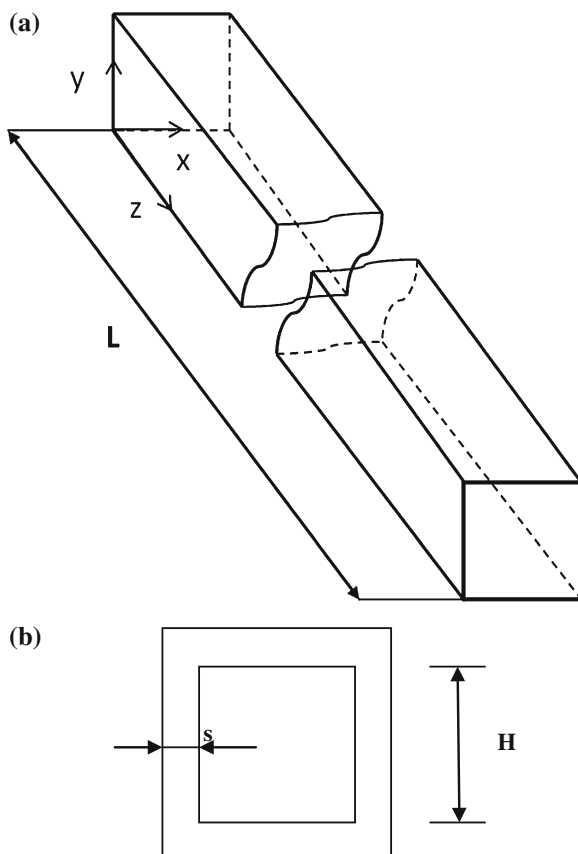

Table 1 Thermophysical properties of cordierite

ρ [kg/m^3]	c [J/kg K]	k [W/m K]
2,300	900	2.5

Table 2 Heat transfer coefficients

Porosity, φ	h [W/m^{2}K] without radiation	h [W/m^{2}K] with radiation $\varepsilon = 0.9$
0.9	39.6	48.5
0.3	35.2	45.5
0.1	29.0	33.1

Different charging-discharging cycles are considered. In the charging phase the gas enters at 1,473 K whereas in discharging phase it enters countercurrent at 1,073 K. The charge, in the first cycle, starts with the heat storage system temperature set at 300 K and, in some cases ends when 90 % of maximum storable

energy, in this cycle, is reached. Then the discharging phase starts and the cycle ends when the outlet gas temperature reaches 1,173 K. The same criteria are utilized in the second cycle that starts with the heat storage system temperature set at 1,073 K.

3 Results

First results are presented for storage obtained by a porous medium. Two different porous media are considered: spheres or foams. In all cases a ceramic material is considered. For packed bed configuration, the results are presented in terms of stored energy profiles for cordierite spheres. Five porosity values are analyzed in ranging from 0.2 to 0.6, mass flow per unit cross section, G, inlet has values equal 0.1, 0.2, and 0.3 kg/m²s for all cases.

In Fig. 7, energy stored is reported as a function of time, for ε values in the range from 0.2 to 0.6 and G equal to 0.1 kg/m²s, for charge and discharge cycles. Decreasing the porosity the charging and discharging time increases due to the thermal capacity increase. Increasing the porosity value steady state conditions are reached at lower time both in charging and discharging phases.

In Figs. 8 and 9, stored thermal energy as a function of time is depicted for mass flow per unit cross section equal to 0.2 and 0.3 kg/m²s. It is noted that the steady state is attained at lower time value due to a more efficient convective heat transfer between the fluid and the solid matrix. However, increasing the mass flow rate the energy level, in the case with adiabatic external surface of the storage, any variation in the energy stored values is detected. In this case, the main result is that charging and discharging times decrease as the mass flow rate increases.

Also for ceramic foam configuration, the results are presented in terms of energy stored profiles.
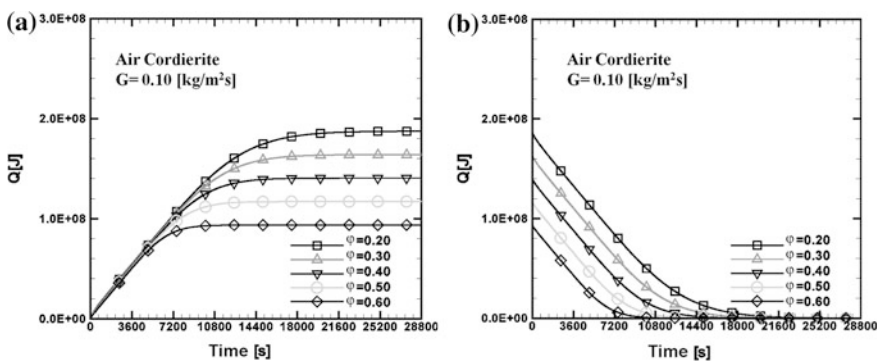

Fig. 7 Energy stored for several porosity values and G equal to 0.10 kg/m²s: **a** charge cycle, **b** discharge cycle

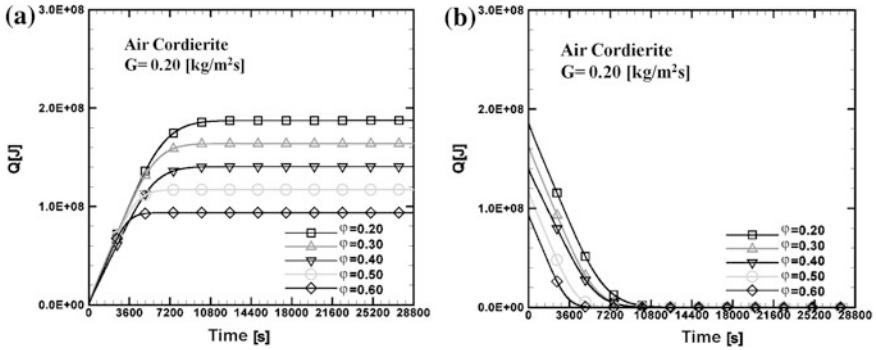**Fig. 8** Energy stored for several porosity values and G equal to 0.20 kg/m²s: **a** charge cycle, **b** discharge cycle

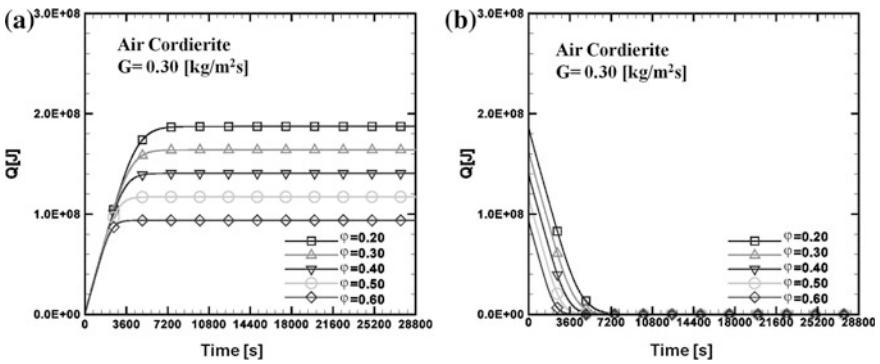**Fig. 9** Energy stored for several porosity values and G equal to 0.30 kg/m²s: **a** charge cycle, **b** discharge cycle

Alumina foam with porosity equal to 0.858 and 20 PPI is investigated. For charge phase the initial temperature of solid is equal to 300 K while at inlet the temperature is equal to 1,473 K. In the discharge phase the air has the inlet section opposite at the one in the charge phase and the inlet temperature is 1,073 K. In this configuration also the effect of heat transfer losses is analyzed. For all studied configurations, the heat transfer coefficient on the external surface of cylinder is assumed equal to 5 W/m²K. Three different mass flow rates are analyzed and they are equal to 0.050, 0.10 and 0.20 kg/s. For mass flow rate equal to 0.20 kg/s also the case with radiative heat transfer is analyzed.

Figure 10 shows stored energy profiles as a function of time for adiabatic and with heat losses cases. When mass flow per unit cross section increases charging and discharging times decrease. Steady state conditions are reached in any case. It is noticed that for the cases with heat transfer losses with an external heat transfer coefficient equal to 5.0 W/m²K, the energy stored value is lower than the adiabatic
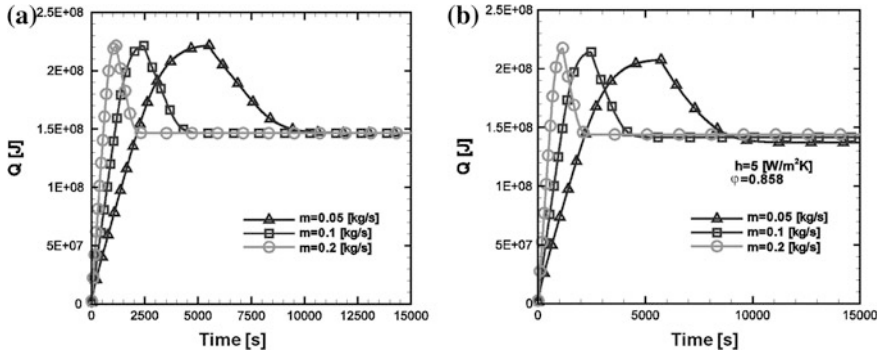
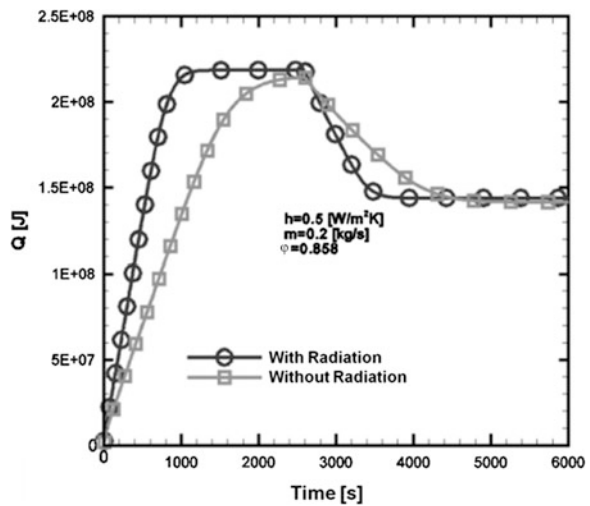**Fig. 10** Energy stored for several mass flow rate values and porosity equal to 0.858: **a** adiabatic case, **b** h = 5 W/m² K

Fig. 11 Energy stored for mass flow rate value equal to 0.2 kg/s and porosity equal to 0.858 with and without radiative heat transfer

ones. In Fig. 11 the effect of radiation heat transfer mechanism is showed. The stored energy stored are the same for both configurations studied, but for configuration with radiation heat transfer charging and discharging time decrease.

In the following results are presented for porosity equal to 0.395, spheres diameter equal to 0.010, 0.025, and 0.040 m. Mass flow inlet has values equal to 0.05, 0.10, and 0.20 kg/s for all cases.

In Fig. 12 thermal energy stored, volumetric fluid and solid average temperature are shown as function of time, for $\varphi = 0.395$ and $d_p = 0.025$ m, for the first cycle. At the increase of mass flow rate, charging and discharging time decrease. Regime condition is not reached for any case. The stored thermal energy is 200 and 50 kWh are released during the discharge phase as quickly as the mass flow rate increases.
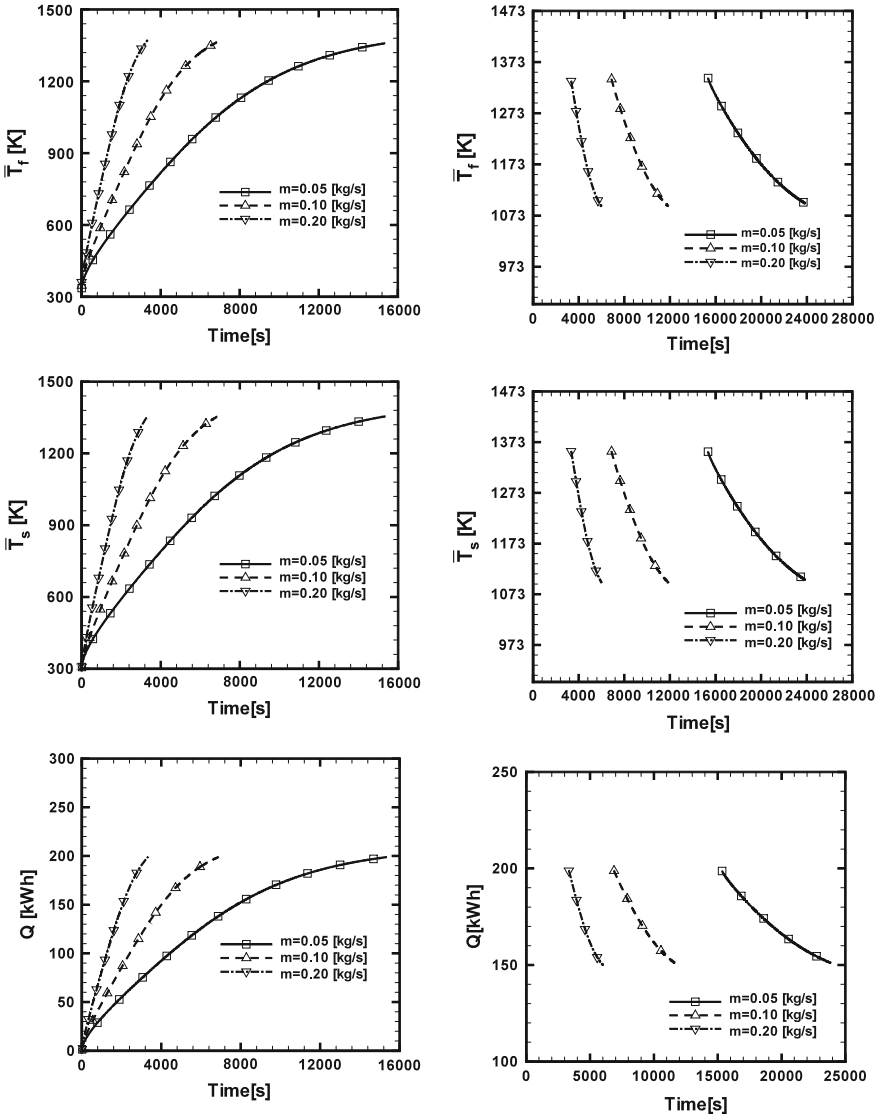
Fig. 12 Thermal energy stored, volumetric fluid and solid average temperature for $\varphi = 0.395$, $d_p = 0.025$ m, first cycle

In Fig. 13 thermal energy stored, volumetric fluid and solid average temperature are shown as function of time, for $\varphi = 0.395$, $d_p = 0.025$ m, for the second cycle. At the increase of mass flow rate, charging and discharging time decrease. Charging and discharging time increase compared to the first cycle. Regime condition is reached only for mass flow rate equal to 0.05 kg/s during the charging
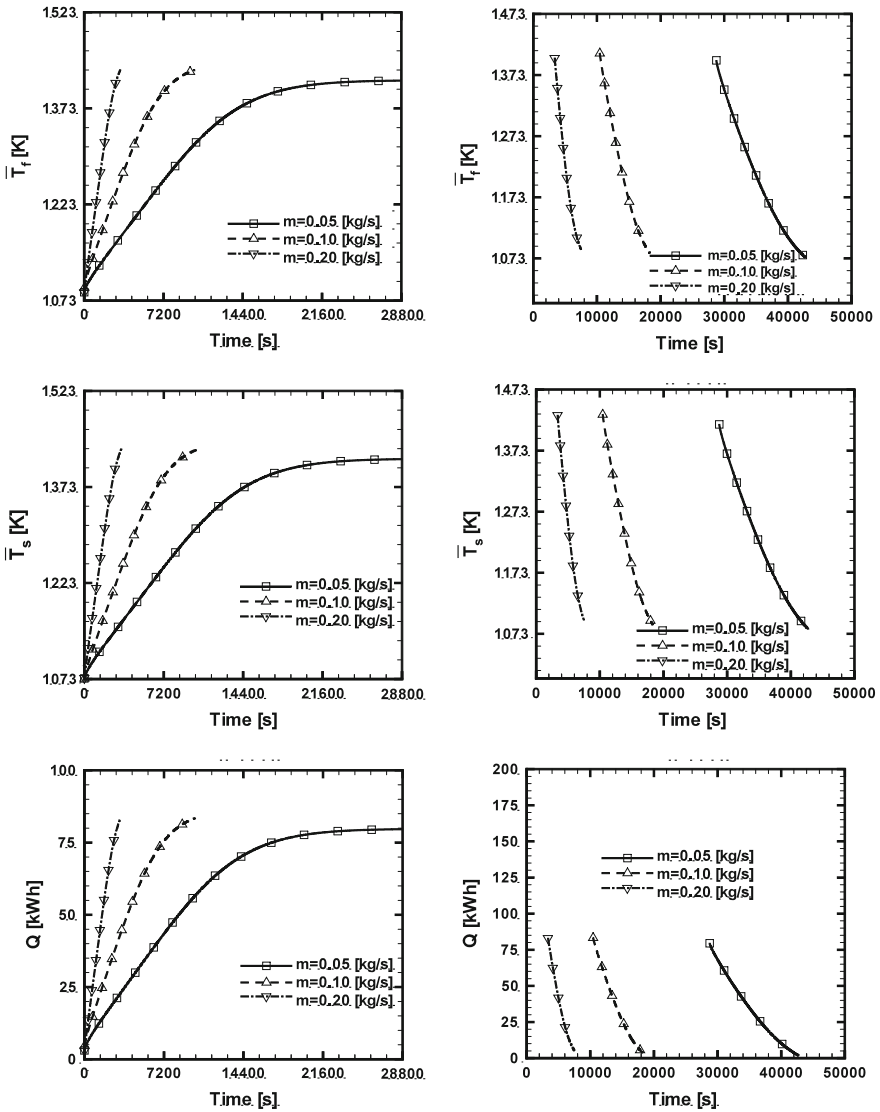
Fig. 13 Thermal energy stored, volumetric fluid and solid average temperature for $\varepsilon = 0.395$, dp = 0.025 m, second cycle

phase. The energy stored value is lower than that corresponding to the stop rate, charging and discharging time decrease. The energy stored value is lower than that corresponding to the stop value. The stored thermal energy is 80 kWh for mass flow rate equal to 0.05 kg/s and is 85 kWh for m = 0.10 kg/s and for m = 0.20 kg/s. This energy is completely released during the discharge phase as quickly as the mass flow rate increases.

Table 3 Second-law efficiency for packed bed configuration $\varphi = 0.395$

	I cycle			II cycle		
	Mass flow rate [kg/s]			Mass flow rate [kg/s]		
Sphere diameter [m]	0.05	0.10	0.20	0.05	0.10	0.20
0.010	0.126	0.198	0.246	0.050	0.309	0.434
0.025	0.120	0.187	0.200	0.085	0.171	0.391
0.040	0.113	0.150	0.163	0.065	0.124	0.228
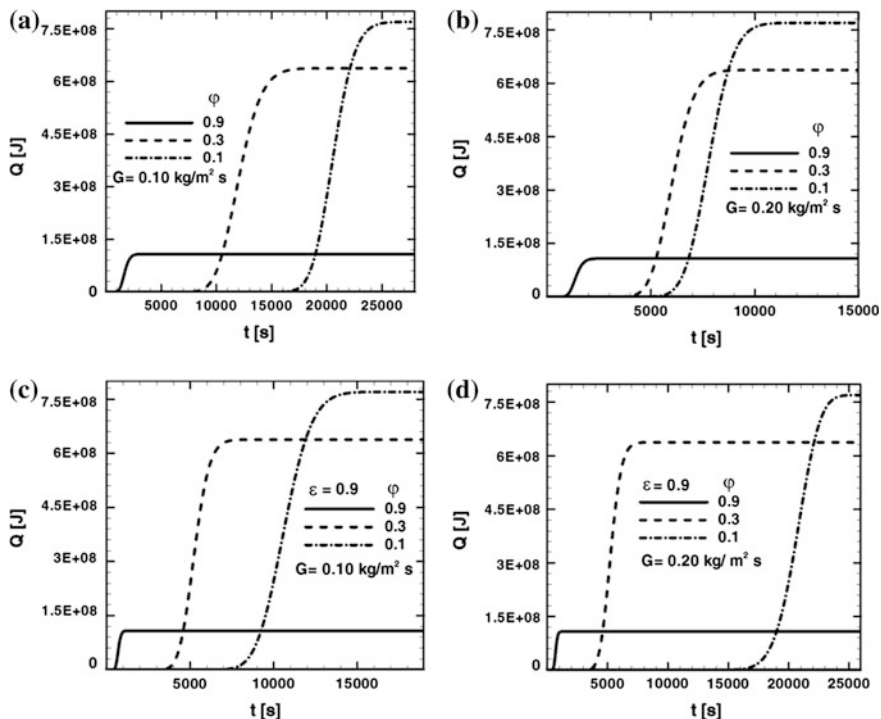
Fig. 14 Stored energy for different porosity values and mass flow; G = **a** 0.1 kg/m^{2}s and without radiation effect; **b** 0.2 kg/m^2 s and without radiation effect; **c** 0.1 kg/m^{2}s and $\varepsilon = 0.9$; **d** 0.2 kg/m^{2}s and $\varepsilon = 0.9$

In Table 3, second-law efficiency of analyzed TES [59], in packed bed configuration is shown. It is noted that TES efficiency decreases increasing d_p and decreasing mass flow rate. II Cycle TES efficiency values are, generally, higher than the I Cycle ones. In this cycle only for mass flow rate equal to 0.05 kg/s TES efficiency values are less than the corresponding values of the first cycle. This is due to the system impossibility to reach stop condition in the charging phase.

Table 4 Energy stored values

φ	Q [J]
0.9	1.2×10^8
0.3	6.4×10^8
0.1	7.7×10^8

For the Honeycomb solid matrix results are presented in terms of thermal energy stored. Two different mass velocity, G, equal to 0.1 and 0.2 kg/m^{2}s are studied for three porosities equal to 0.1, 0.3 and 0.9, the effects of radiation are taken into account for all configurations studied, the emissivity is set equal to 0.9. The analysis takes into account the outlet section to evaluate the charging time i.e., the time at which the outlet section reaches the inlet fluid temperature and the steady state is reached.

Figure 14a and b show stored thermal energy as a function of time for assigned porosity values equal to 0.9, 0.3 and 0.1, and mass flow values equal to 0.1 and 0.2 kg/m^2 s, without radiation heat transfer effects. Decreasing the porosity the charging time increases due to the thermal capacity increase. Increasing the porosity value steady state conditions are reached at lower time for the charging phase. However, increasing the mass flow rate any variation in the stored energy values is detected. As expected, for assigned mass flow rate, the porosity value determines also the stored energy level whereas, for assigned porosity, the mass velocity or the mass flow rate affects the charging time of the system.

In Fig. 14c and d the radiative effects on stored thermal energy are observed. In fact, considering radiation heat transfer, any variation in stored energy values is detected but the charging time decreases.

The stored energy values at steady state condition are summarized in Table 4. It is observed that an increase of the stored energy of about 5 times is obtained passing from the porosity value equal to 0.9 to a value of 0.3 whereas passing from 0.9 to 0.1 the increase is about 6.4 times.

Figure 15 depicts the temperature behavior for charge and discharge cycle for a porosity equal to 0.9, mass flow rate per unit section area equal to 0.1 and 0.2 with and without radiation effect. The charging and discharging times decrease increasing the mass flow rate. The presence of radiative heat transfer in the porous medium determines a decrease in charging and discharging times. At decreasing of porosity charge and discharge times increase, according to the previous presented results.
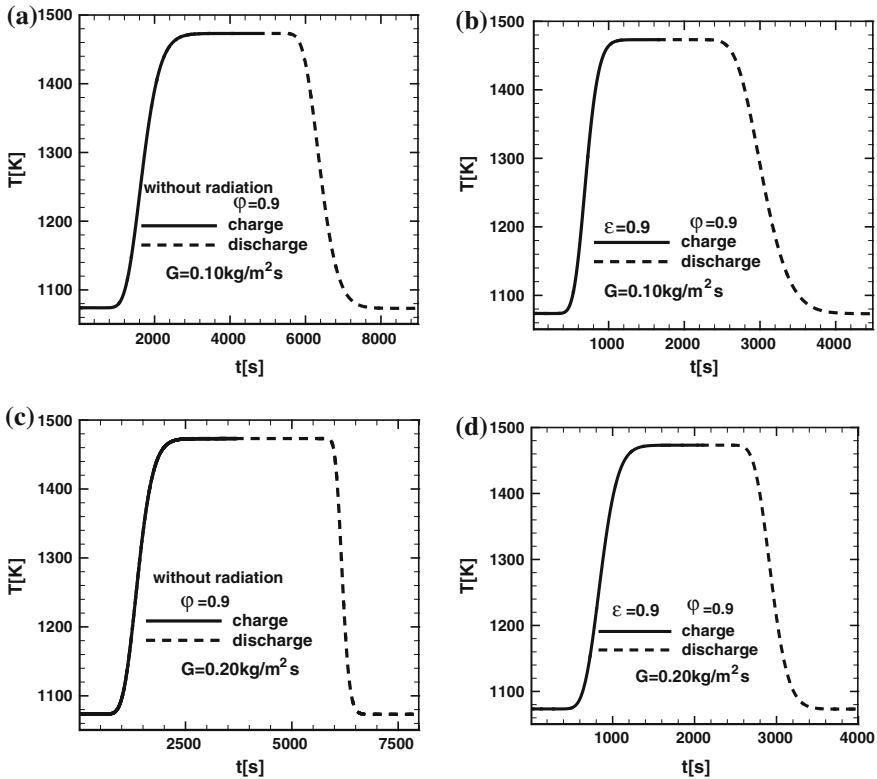
Fig. 15 Temperature profiles for porosity equal to 0.9 and **a** G = 0.1 kg/m²s; **b** G = 0.1 kg/m²s and ε = 0.9 **c** G = 0.2 kg/m²s; **d** G = 0.2 kg/m²s and ε = 0.9

4 Conclusions

Thermal behavior of high temperature sensible heat thermal energy storage system with different solid matrixes in cylindrical container was analyzed. The governing equations were written employing the Brinkman-Forchheimer-Darcy model in local thermal non equilibrium. The study was performed in the charge and discharge phases, analyzing the effect of packed bed with ceramic spherical particles, ceramic foams and honeycomb structure with square transversal section channels. Results in terms of temperature profiles of outlet section as a function of time allowed to determine the effects of porosity, mass flow rate and the radiation on the complete charge and discharge time. The heat losses and the presence of radiative heat transfer in porous medium determined an increase in charge and discharge times. The main effect was due to the porosity which determined also the thermal energy storage value. An optimal porosity value could be evaluated taking into account also the pressure drop and the viscous dissipation inside the system.

References

1. Dell, R., Rand, D.: Energy storage—a key technology for global energy sustainability. J. Power Sources **100**, 2–17 (2001)
2. Dincer, I., Rosen, M.: Thermal energy storage: System and application. Wiley, New York (2002)
3. Beckmann, G., Gilli, P.V.: Thermal energy storage: Basics, design applications to power generation and heat supply. Springer, Heidelberg (2002)
4. Paksoy, H.Ö.: Thermal energy storage for sustainable energy consumption: Fundamentals case studies and design. Springer, Heidelberg (2007)
5. Arteconi, A., Hewitt, N.J., Polonara, F.: State of the art of thermal storage for demand-side management. Appl. Energy **93**, 371–389 (2012)
6. Oró, E., Gil, A., de Gracia, A., Boer, D., Cabeza, L.F.: Comparative life cycle assessment of thermal energy storage systems for solar power plants. Renew. Energy **44**, 166–173 (2012)
7. Lia, P., Van Lew, J., Chan, C., Karaki, W., Stephens, J., O'Brien, J.E.: Similarity and generalized analysis of efficiencies of thermal energy storage systems. Renew. Energy **39**, 388–402 (2012)
8. Zanganeh, G., Pedretti, A., Zavattoni, S., Barbato, M., Steinfeld, A.: Packed-bed thermal storage for concentrated solar power—pilot-scale demonstration and industrial-scale design. Sol. Energy **86**, 3084–3098 (2012)
9. Calvet, N., Gomez, J.C., Faik, A., Roddatis, V.V., Meffre, A., Glatzmaier, G.C., Doppiu, S., Py, X.: Compatibility of a post-industrial ceramic with nitrate molten salts for use as filler material in a thermocline storage system. Appl. Energy http://dx.doi.org/10.1016/j.apenergy.2012.12.078 (2013)
10. Singh, H., Saini, R.P., Saini, J.S.: A review on packed bed solar energy storage systems. Renew. Sust. Energy Rev. **14**, 1059–1069 (2010)
11. Sharma, A., Tyagi, V.V., Chen, C.R., Buddhi, D.: Review on thermal energy storage with phase change materials and applications. Renew. Sust. Energy. Rev. **13**, 318–345 (2009)
12. Gil, A., Medrano, M., Martorell, I., Lazaro, A., Dolado, P., Zalba, B., Cabeza, L.: State of the art on high temperature thermal energy storage for power generation. Part1—concepts, materials, and modellization. Renew. Sust. Energy Rev. **14**, 31–55 (2010)
13. Hänchen, M., Brückner, S., Steinfeld, A.: High-temperature thermal storage using a packed bed of rocks—heat transfer analysis and experimental validation. Appl. Thermal Eng. **31**, 1798–1806 (2011)
14. Powell, K.M., Edgar, T.F.: Modeling and control of a solar thermal power plant with thermal energy storage. Chem. Eng. Sci. **71**, 138–145 (2012)
15. Liu, M., Saman, W., Bruno, F.: Review on storage materials and thermal performance enhancement techniques for high temperature phase change thermal storage systems. Renew. Sust. Energy Rev. **16**, 2118–2132 (2012)
16. Fernandes, D., Pitié, F., Cáceres, G., Baeyens, J.: Thermal energy storage: "How previous findings determine current research priorities". Energy **39**, 246–257 (2012)
17. DeLaquil, P., Kelly, B., Lessley, R.: Solar one conversion project. Sol. Energy Mater. **24**, 151–161 (1991)
18. Herrmann, U., Kearney, D.W.: Survey of thermal energy storage for parabolic trough power plants. ASME J. Sol. Energy Eng. **124**, 145–152 (2002)
19. Steinmann, W.D., Eck, M.: Buffer storage for direct steam generation. Sol. Energy **80**, 1277–1282 (2006)

20. Tamme, R., Laing, D., Steinmann, W.D.: Advanced thermal energy storage technology for parabolic trough. ASME J. Sol. Energy Eng. **126**, 794–800 (2004)
21. Watanabe, T., Kikuchi, H., Kanzawa, A.: Enhancement of charging and discharging rates in a latent heat storage system by use of PCM with different melting temperatures. Heat Rec. Syst. CHP **13**, 57–66 (1993)
22. Lovegrove, K., Luzzi, A., Soldiani, I., Kreetz, H.: Developing ammonia based thermochemical energy storage for dish power plants. Sol. Energy **76**, 331–337 (2004)
23. Meier, A., Winkler, C., Wuillemin, D.: Experiment for modelling high temperature rock bed storage. Sol. Energy Mater. **24**, 255–264 (1991)
24. Bader, R., Pedretti, A., Steinfeld, A.: A 9-m-aperture solar parabolic trough concentrator based on a multilayer polymer mirror membrane mounted on a concrete structure. ASME J. Sol. Energy Eng. **133**, 031016 (2011)
25. Coutier, J.P., Farber, E.A.: Two applications of a numerical approach of heat transfer process within rock beds. Sol. Energy **29**, 451–462 (1982)
26. Schumann, T.E.W.: A liquid flowing through a porous prism. J. Franklin Inst. **28**, 405–416 (1929)
27. Klinkenberg, A.: Numerical evaluation of equations describing transient heat and mass transfer in packed solids. Ind. Eng. Chem. **40**, 1992–1994 (1948)
28. Ledoux, E.: Dynamic cooling at absorbent beds. Ind. Eng. Chem. **40**, 1970–1975 (1948)
29. Larsen, F.W.: Rapid calculation of temperature in a regenerative exchanger having arbitrary initial solid and fluid temperatures. Int. J. Heat Mass Transfer **10**, 149–168 (1967)
30. Duffie, J.A., Beckman, W.A.: Solar energy thermal processes. Wiley, New York (1974)
31. Klein, S.A.: Mathematical models at thermal storage. Proceedings of solar energy storage subsystems for the heating and cooling of building, pp. 119–128 (1975)
32. Mumma, S.A., Marvin W.C.: A method of simulating the performance of a pebble bed thermal energy storage and recovery system. ASME-AICHE heat transfer conference 1986, St. Louis, paper 76 -HT-73 (1976)
33. Saez, A.E., McCoy, B.J.: Dynamic response of a packed bed thermal storage system-a model for solar air heating. Sol. Energy **29**, 201–206 (1982)
34. Dincer, I., Dost, S., Li, X.: Performance analysis of sensible heat storage systems for thermal applications. Int. J. Energy Res. **21**, 1171–1257 (1997)
35. Fath, H.E.: Technical assessment of solar thermal energy storage technologies. Renew. Energy **14**, 35–40 (1998)
36. Ismail, K.A.R., Stuginsky Jr, R.: A parametric study on possible fixed bed models for PCM and sensible heat storage. Appl. Thermal Eng. **19**, 757–788 (1999)
37. Crandall, D., Thacher, E.: Segmented thermal storage. Sol. Energy **77**, 435–440 (2004)
38. Singh, R., Saini, R.P., Saini, J.S.: Nusselt number and friction factor correlations for packed bed solar energy storage system having large sized elements of different shapes. Sol. Energy **80**, 760–771 (2006)
39. Singh, C., Tathgir, R.G., Muralidhar, K.: Energy storage in fluid saturated porous media subjected to oscillatory flow. Heat Mass Transfer **45**, 427–441 (2009)
40. Andreozzi, A., Buonomo, B., Dongiacomo, V., Manca, O., Mesolella P.: Numerical analysis on different sensible thermal energy storage component in high temperature solar systems. Proceedings of heat-SET conference on heat transfer in components and systems for sustainable energy technologies, pp. 21–29, Opatija, Croatia, Edition GRETh, France, 20–21 Oct 2010
41. Lu, T.J.: Heat transfer efficiency of metal honeycombs. Int. J. Heat Mass Transfer **42**, 2031–2040 (1998)
42. Rafidi, N., Blasiak, W.: Thermal performance analysis on a two composite material honeycomb heat regenerators used for HiTAC burners. App. Thermal Eng. **25**, 2966–2982 (2005)
43. Tescari, S., Neveu, P., Mazet, N.: Thermochemical solar reactor: Simplified method for the geometrical optimization at a given incident flux. Int. J. Chem. Reactor Eng. **8**, art. no. A24 (2010)

44. Luo, X., Liu, Y., Liu, W.: A honeycomb microchannel cooling system for microelectronics cooling. Heat Transfer Eng. **32**, 616–623 (2011)
45. Bhouri, M., Goyette, J., Hardy, B.J., Anton, D.L.: Honeycomb metallic structure for improving heat exchange in hydrogen storage system. Int. J. Hydrogen Energy **36**, 6723–6738 (2011)
46. Liu, Y., Chen, X., Liu, R.: Numerical simulation of heat transfer and gas flow characteristics in honeycomb ceramics. Adv. Mat. Res. **156–157**, 984–987 (2011)
47. Krishnan, S., Hernon, D., Hodes, M., Mullins, J., Lyons, A.M.: Design of complex structured monolithic heat sinks for enhanced air cooling. IEEE Trans. Comp. Packag. Manuf. Tech. **2**(6111210), 266–277 (2012)
48. Han, X.H., Wang, Q., Park, Y.G., T'Joen, C., Sommers, A., Jacobi, A.: A review of metal foam and metal matrix composites for heat exchangers and heat sinks. Heat Transfer Eng. **33**, 991–1009 (2012)
49. Dhall, A., Squier, G., Geremew, M., Wood, W.A., George, J., Datta, A.K.: Modeling of multiphase transport during drying of honeycomb ceramic substrates. Drying Tech. **30**, 607–618 (2012)
50. Andreozzi, A., Buonomo, B., Manca, O., Tamburrino, S.: Thermal energy storages analysis for high temperature in air solar systems, submitted to ASME J. Sol. Energy Eng. (2013)
51. Andreozzi, A., Buonomo, B., Manca, O., Mesolella, P., Tamburrino, S.: Numerical investigation on sensible thermal energy storage with porous media for high temperature solar systems. J. Physics: Conf. Series **395**, paper no. 012150, doi:10.1088/1742-6596/395/1/012150 (2012)
52. Vafai, K.: Handbook of Porous Media. Marcel Dekker, New York (2000)
53. Jeng, T.M., Tzeng, S.C.: Numerical study of confined slot jet impinging on porous metallic foam heat sink. Int. J. Heat Mass Transfer **48**, 4685–4694 (2005)
54. Vafai, K.: Convective flow and heat transfer in variable-porosity media. J. Fluid Mech. **147**, 233–259 (1984)
55. Dullien, F.A.L.: Porous Media Fluid Transport and Pore Structure. Academic, San Diego (1979)
56. Vafai, K., Sozen, M.: Analysis of energy and momentum transport for fluid flow through a porous bed. ASME J. Heat Transfer **112**, 690–699 (1990)
57. Moreira, E.A., Innocentini, M.D.M., Coury, J.R.: Permeability of ceramic foams to compressible and incompressible flow. J. Eur. Ceram. Soc. **24**, 3209–3218 (2004)
58. Zhao, C.Y., Tassou, S.A., Lu, T.J.: Analytical considerations of thermal radiation in cellular metal foams with open cells. Int. J. Heat Mass Transfer **51**, 929–940 (2008)
59. Adebiyi, G.A., Hodge, B.K., Steele, W.G., Jalalzadeh-Aza, A., Nsofor, E.C.: Computer simulation of a high-temperature thermal energy storage system employing multiple families of phase change storage material. ASME J. Energy Res. Tech. **118**, 102–111 (1996)